Picking up good vibrations

Exploration of the intensified vibratory mill via a modern design of experiments

De Cleyn, Elene; Holm, René; Khamiakova, Tatsiana; Van den Mooter, Guy

Published in:
International Journal of Pharmaceutics

DOI:
10.1016/j.ijpharm.2021.120367

Publication date:
2021

Document Version
Peer reviewed version

Citation for published version (APA):
De Cleyn, E., Holm, R., Khamiakova, T., & Van den Mooter, G. (2021). Picking up good vibrations: Exploration of the intensified vibratory mill via a modern design of experiments. *International Journal of Pharmaceutics*, *598*, Article 120367. https://doi.org/10.1016/j.ijpharm.2021.120367

Picking up good vibrations:

Exploration of the intensified vibratory mill via a modern Design of Experiments.

Contact:

Elene De Cleyn[1], René Holm[2, 3], Tatsiana Khamiakova[4], Guy Van den Mooter[1*]

[1] Drug delivery and Disposition, Department of Pharmaceutical and Pharmacological Sciences, University of Leuven (KU Leuven), O&N II Herestraat 49 - box 921, 3000 Leuven, Belgium

[2] Drug Product Development, Janssen Research and Development, Johnson and Johnson, Turnhoutseweg 30, 2340 Beerse, Belgium

[3] Department of Science and Environment, Roskilde University, 4000 Roskilde, Denmark

[4] Quantitative Sciences, Janssen Research and Development, Johnson and Johnson, Turnhoutseweg 30, 2340 Beerse, Belgium

*Correspondence;

Guy Van den Mooter

O&N II Herestraat 49 -box 921, 3000 Leuven, Belgium

guy.vandenmooter@kuleuven.be,

tel.+32 16 33 03 04

tel. +32 473 356 132

Graphical abstract

Key words

Design of Experiments

Intensified vibratory milling

Method optimisation

Milling

Particle size reduction

Quality by Design

Abbreviations

API: Active pharmaceutical ingredient

DoE: Design of Experiments

E_{kin}: Kinetic energy

GM: Grinding media

iRI: Imaginary part of the complex refractive index

IVM: Intensified vibratory milling

LD: Laser diffraction

N_C: Number of contact moments between beads

Obsc: Red light obscuration

Obsc. blue.: Blue light obscuration

PSD: Particle size distribution

REML: Restricted maximum likelihood

Res.: Residuals

Res. weight.: Residuals Weighted

RMSE: Root Mean Square Error

rRI: Real part of the complex refractive index

SF: Stress frequency

SI_{GM}: Stress intensity of the grinding media

SN: Stress number

WBM: Wet bead milling

Abstract

The aim of this work was to strengthen the understanding of the intensified vibratory mill by unravelling the milling process in terms of the particle size reduction and heat generation via a modern design of experiments approach. Hence, the influence of five process parameters (acceleration, breaks during milling, bead size, milling time and bead-suspension ratio) was investigated via an I-optimal design. Particle size was measured via laser diffraction and the temperature of the sample after milling was computed. To advance our understanding, a mechanistic model for the set-up of wet-stirred media milling processes was applied on the observed milling trends. A generic approach for the optimisation of the milling process was retrieved and included the optimisation of the bead size and intermittent pausing for effective cooling. To finetune the remaining process parameters, the present work provides contour plots and strong predictive models. With these models, the particle size and the temperature after milling of suspensions manufactured with the intensified vibratory mill could be forecasted for the first time.

1. Introduction

Micronisation and nanonisation are commonly applied approaches to enable the bioavalability of poorly water soluble compounds by enhancing their solubility and/or dissolution rate. (Li et al., 2016a) Formulated as a nano- or microsuspension, these poorly soluble compounds may be delivered via a variety of administration routes including the oral, ocular, brain, topical, buccal, nasal and transdermal routes. (Jacob et al., 2020) By virtue of their ease of use, suspensions can be orally administrated in wet state or after incorporation into conventional dosage forms such as tablets or capsules. (Malamatari et al., 2016) Injectable nano- and micro suspensions have drawn increasing attention due to their potential use as long-acting injectables. (Sigfridsson et al., 2019) This formulation type can offer great utility for chronic diseases, where lack of medication compliance may be detrimental for the pharmacological response. (Owen and Rannard, 2016). Overall, advancements in the production and formulation of these suspensions can solve numerous pharmacokinetic challenges and these topics are therefore still heavily studied. (Jacob et al., 2020)

Among all the usable production technologies, wet bead milling (WBM) is most widely applied with demonstrated efficiency, viability and cost-effectiveness at production scale. (Merisko-Liversidge and Liversidge, 2011), (Li et al., 2016a). Milling media, dispersant, stabilizer, other excipients and the active pharmaceutical ingredient (API) are charged into the milling chamber and by the movement of the milling media, shear forces, pressure and impact are generated, leading to a particle size reduction. Either the milling beads are accelerated by the movement of the complete container, or by agitators installed in the chamber. (Müller and Junghanns, 2008) Extensive ball milling to the nanorange was patented as the Nanocrystal® Technology by Elan, in 1990 (Müller et al., 2001), a technology that led to many (sub)micronized drug products of poorly soluble APIs on the market. (Jacob et al., 2020) Opportunities for milling on bench-level are numerous, such as the high-throughput platforms, streamlining formulation screening and optimization. (Van Eerdenbrugh et al., 2009) The technologies' major drawback is the heat generated by inefficiently dissipated energy wherefore a water jacket is more often installed. Yet, WBM is considered as the golden standard for nanonisation and micronisation. However, this enabling platform still encounters some unresolved issues. These include erosion of the milling media which

may contaminate the final formulation (Li et al., 2016a) and extensive milling times from several hours to days (Müller et al., 2001).

Consequently, new milling technologies such as the intensified vibratory mill (IVM) in which the ResonantAcoustic® Mixing platform is used, are introduced in the field. Originally commercialised as a mixing platform, the ResonantAcoustic® Mixing platform has been mostly employed as a dry mixing process, whereas its application in wet milling is less studied. (Li et al., 2016b), (Leung et al., 2014) As a milling platform, it consists of a closed vibrating container to which milling media are charged. The vibrating container could be of various types of vessels, vials or well-plates. In this way, the IVM could serve as a drug sparing, high-throughput screening method. (Leung et al., 2014) The vibration can be described as a sinusoidal wave with a frequency of around 60 Hz, as to keep the system at its optimal and safe conditions, the parametric resonance. The amplitude of the sinusoidal wave on the other hand differs, based on the milling content and the set acceleration. Previously, the mixing behaviour was introduced as micro-mixing zones, but current knowledge seems to present a more complex mixing and milling regime. (Resodyn acoustic mixers, 2018) Insights in milling regimes and the motion of grinding bodies in conventional mills have already been broadly discussed in the literature. (Raasch, 1992), (Blecher et al., 1996) Concerning later mill types, Hagedorn and colleagues have discussed how virtually all beads accelerate as ‘one cloud’ (cloud milling) in the dual centrifuge. (Hagedorn et al., 2017). Since the geometry and the motion of IVMs milling chamber significantly differ from conventional and later mill types, one can assume a different bead motion. Consequently, the extent and distribution of milling forces will differ, leading to a different milling process in terms of particle size reduction and heat generation.

In this viewpoint, IVM has been marked for its fast particle size reduction which can overcome the extensive milling times, encountered in classical WBM. Yet unacceptable high temperatures have been observed. (De Cleyn et al., 2020) First attempts to control this temperature included the installation of milling breaks in which the containers were removed from the milling equipment and placed in a refrigerated bath. (Li et al., 2016b) This method proved to be effective, but difficult to standardize or scale-up. Further, the influence of this quick cooling step on the aggregation of particles and recrystallisation of dissolved API was not explored. Consequently, the purpose of this study was to obtain a comprehensive insight in the process of particle

size reduction and heat generation as it applies to IVM, with the usage of a design of experiments (DoE).

To the best of our knowledge, publications on the usage of DoE methodologies within pharmaceutical milling are limited to classical designs such as the central composite or (fractional) factorial designs (Peltonen, 2018). In order to reach predictive models of similar quality and precision, modern DoE methodologies allow to simultaneously study many factors in an irregular experimental domain in an economic fashion.(de Aguiar et al., 1995) (Jensen, 2018) Surprisingly, the application of modern DoE methodologies on pharmaceutical milling is so far unexplored. Moreover, no previous study on the investigation of IVM via a DoE, classical or modern, has, to the best of our knowledge, been published.

In this work, a novel DoE methodology was applied to generate deep insights in the heat generation and nanosizing potential of the IVM. The selected I-optimal design and consecutive statistical analysis ranked the investigated process parameters (bead size, breaks during milling, acceleration, milling time and bead-suspension ratio), elucidated interactions between these parameters and provided a predictive model for important suspension attributes such as the dv50-value, dv90-value, particle size distribution (span) and temperature after milling. To gain more mechanistic insight in the milling kinetics, the stress model (Kwade, 1992) was applied on the milling trends and questions regarding the impact of pausing on heat generation and particle size, were addressed.

2. Methods and materials

2.1. Materials

Bedaquiline was provided by Janssen Pharmaceutica (Beerse, Belgium). Polysorbate 20 was obtained from Croda (Trappes, France). Deionized water (R≥18.2 MΩ, Mili-Q® Advantage A10, Merck, Darmstadt, Germany) was used for all the experiments.

2.2. Methods

2.2.1. Preparation of suspensions

Glass vials were filled with bedaquiline (5% w/v), zirconia beads (Nikkato Corporation, Sakai, Osaka, Japan) and Polysorbate 20 solution (1.85 %w/v). The vials were thoroughly shaken on an in-house manufactured platform within the LabRAM II (Resodyn Acoustic Mixers, Butte, USA). The investigated process parameters - the acceleration, the bead size, the bead-suspension ratio, the milling time and the breaks during milling - were varied as proposed in the DoE (Fig. 1).

2.2.2. Experimental design

The acceleration, the bead size, the bead-suspension ratio and the milling time were, as earlier demonstrated (De Cleyn et al., 2020), explorable parameters that could impact the output of the milling process in terms of the suspension's final particle size and temperature. In attempt to control the temperature, an additional parameter, named 'Breaks during milling', was included. This parameter encompassed the duration of the installed break (0 minutes, 2.5 minutes or 5 minutes), implemented every 7.5 minutes of the milling process.

Within the Jump software package (JMP® 13.0.0, SAS Institute Inc.), a custom DoE was built in which the five process parameters were set as quantitative, continuous parameters with an upper and lower limit based on historical data. To enhance the predictive power and the robustness of the model, two centre points and four replicates were included. Blocking was applied and experiments were randomized. Chosen responses were the median particle size (dv50), the particle size distribution (PSD) (dv90, span) and the final temperature of the suspension (Temp.). In order to broadly explore the complexity of the milling process, 22 model parameters were selected for investigation. These parameters included the intercept, all main effects, all two-way interactions, all quadratic effects, and one three-way interaction (acceleration/bead-

suspension ratio/bead size). For a classical DoE with five factors, high-resolution designs would be required to resolve such three-factor interaction. Nonetheless, the final experimental design, generated with the JMP® software, was a three level I-optimal design with 30 experimental runs, which covered the whole experimental domain (Fig. 1).

2.2.3. Temperature measurement

After production, the temperature decline of the suspension was tracked with a temperature gun (VWR® Traceable® Infrared Thermometer, Radnor, PA, US), as presented previously (De Cleyn et al., 2020). The temperature directly after milling was obtained by extrapolation of the tracked temperature trend.

2.2.4. Laser diffractometry

Laser diffraction (LD) measurements were performed on a Mastersizer™ 2000 (Malvern Instruments, Worcestershire, UK) with hydro-unit, using miliQ water as the dispersant. Stirring speed of 600 rpm was set, no sonication was applied, and the system was left to stabilize for five minutes. Finally, the system was aligned, and the background was evaluated. The general-purpose model for irregularly shaped particles with normal calculation sensitivity was applied. The set optical parameters were a sample rRI of 1.595, a sample iRI of 0.001 and a dispersant rRI of 1.333. A limited obscuration titration was performed for each sample to elucidate the optimal set of a red light (Obsc.) and blue light obscuration (Obsc. blue). Quality of data was given in terms of residuals (Res.) and residuals weighted (Res Weight.), as described in prior work. (De Cleyn et al., 2019) The final PSD was presented by the dv50-value, the dv90-value and the span (Equation 1).

$$Span = \frac{dv_{90} - dv_{10}}{d_{v50}} \qquad \textit{(Eq. 1)}$$

3. Results

3.1. Design of experiments computation

To deconvolute the individual effects of, and the interactions between the various parameters, the raw data (Table 1) were analysed with the JMP® software. The data were modelled by predictive models with restricted maximum likelihood (REML) to account for the blocking nature of the experiment. REML with unbounded variance components was used for the dv50-value, span and temperature after milling. As the block variance was negligible, REML with bounded variance components was applied on the dv90-value. To get valid statistical estimates, a Bayesian hierarchical model was performed to compute the block variance for the dv90-value (Fig. S1) and to test the significance of the different model parameters (Fig. S2). The block variability approached zero and the same model parameters were significant for the dv90-value, rationalizing the statistical adaptation to bounded variance components.

Predictive models are generally expressed as:

$$Y = \beta_0 + \beta_1 X_1 + \beta_2 X_2 + \beta_3 X_3 + \ldots + \beta_{12} X_1 X_2 + \beta_{23} X_2 X_3 + \beta_{13} X_1 X_3 + \ldots + \beta_{123} X_1 X_2 X_3 + \beta_{11} X_1^2 + \beta_{22} X_2^2 \ldots + \varepsilon \qquad (Eq.\ 2)$$

where Y is the dependent variable or response such as the temperature after milling; $X_1, X_2, X_3 \ldots$ are the independent variables or factors such as milling time; β_0 is the intercept; $\beta_1, \beta_2, \beta_{12}, \beta_{23}, \beta_{123}, \ldots$ are empirically estimated coefficients, better known as the model parameters, which relate the main factors (if the parameters subscript is one digit), interactions (if the parameters subscript is two or more digits) and quadratic effects (if the parameters subscript is two times the same digit) to the forecasted response Y; ε is the total error.

During the interpretation of the significance of the model parameters, the power of the model for these model parameters (Table 2) should be taken into consideration. The power for a certain model parameter, is the probability of the model to detect its significance. The DoE was designed to have an optimal power in the evaluation of all main effects and most two-way interactions. Since the model was restricted to 30 experiments, which was still an elaborated number, the power of the five quadratic effects and of the intercept was rather modest (Table 2). Notwithstanding this modest power, the corresponding model estimates may still have an important effect on the

final responses, independent of statistical significance. For this reason, all model parameters were included in the final predictive models (Model S1, S2, S3 and S4). Overfitting was evaluated by the adjusted determination coefficient (R_{adj}^2).

Table 2: Power analysis of the investigated model parameters. A high power was installed for all main effects and for most two-way-interactions. The power to identify the significance of most quadratic effects and of the intercept, was rather modest.

Parameter	Power
Intercept	0.193
Acceleration (g)	0.932
Breaks during milling (min)	0.897
Milling time (min)	0.869
Bead-suspension ratio	0.776
Bead size (µm)	0.751
Acceleration (g)*Breaks during milling (min)	0.773
Acceleration (g)*Milling time (min)	0.692
Acceleration (g)*Bead-suspension ratio	0.639
Acceleration (g)*Bead size (µm)	0.721
Breaks during milling (min)*Milling time (min)	0.528
Breaks during milling (min)*Bead-suspension ratio	0.721
Breaks during milling (min)*Bead size (µm)	0.818
Milling time (min)*Bead-suspension ratio	0.567
Milling time (min)*Bead size (µm)	0.752
Bead-suspension ratio*Bead size (µm)	0.711
Acceleration (g)*Acceleration (g)	0.247
Breaks during milling (min)*Breaks during milling (min)	0.23
Milling time (min)*Milling time (min)	0.272
Bead-suspension ratio*Bead-suspension ratio	0.24
Bead size (µm)*Bead size (µm)	0.312
Acceleration (g)*Bead-suspension ratio*Bead size (µm)	0.601

Table 1. Process parameters and raw data concerning PSD and temperature after milling, as have been input in the JMP® software

Sample	Process Parameters					Results	PSD			Quality of LD data			
Block 1	**Bead size (µm)**	**Bead/Suspension ratio (mL/mL)**	**Acceleration (g)**	**Total milling time (min)**	**Breaks during milling (min)**	**Temperature (°C)**	**Dv(50) (µm)**	**Dv(90) (µm)**	**Span**	**Obsc**	**Obsc blue**	**Res.**	**Res. Weight.**
Sample 1	200	0.375	50	10	2.5	22.5	21.125	64.279	2.879	9.72	7.63	0.366	0.378
Sample 2	200	1.200	50	10	0	29.5	3.97	40.469	10.109	8.22	9.96	0.442	0.527
Sample 3	1000	0.375	65	20	5	40.1	1.657	4.27	2.484	6.45	7.87	0.589	0.355
Sample 4	200	0.375	80	30	5	39.6	0.637	22.695	35.443	5.59	8.63	0.577	0.419
Sample 5	1000	0.774	80	30	2.5	89.6	0.376	1.746	4.388	5.2	8.21	1.878	1.066
Sample 6	1750	0.375	80	20	0	66.2	1.918	4.924	2.490	4.41	5.43	0.483	0.388
Block 2													
Sample 1	1000	1.200	50	20	2.5	50.2	0.658	2.65	3.871	5.99	6.9	0.403	0.298
Sample 2	1750	0.774	65	10	2.5	50.1	2.046	4.929	2.330	4.64	6.17	0.499	0.386
Sample 3	1750	1.200	80	10	5	78.6	1.34	4.025	2.910	4.89	6.49	0.534	0.349
Sample 4	1750	1.200	80	10	5	78.8	1.283	3.807	2.866	4.64	5.56	0.516	0.485
Sample 5	1750	0.774	65	10	2.5	52.1	1.768	4.152	2.262	4.23	5.9	0.754	0.393
Sample 6	1000	1.200	50	20	2.5	51.9	0.855	2.885	3.240	6.09	8.84	0.703	0.573
Block 3													
Sample 1	200	1.200	80	30	2.5	77.6	0.158	0.433	2.291	2.89	6.79	1.312	1.418
Sample 2	1000	1.200	80	10	0	85.0	0.897	3.088	3.315	4.02	5.66	0.543	0.372
Sample 3	1750	0.774	50	10	5	39.3	1.946	4.509	2.231	4.13	4.91	0.612	0.536
Sample 4	1750	0.375	50	30	2.5	43.8	1.736	4.13	2.300	3.45	4.21	0.69	0.438
Sample 5	1000	0.774	65	20	2.5	60.9	0.682	2.585	3.632	3.13	4.48	0.625	0.74
Sample 6	1750	0.375	50	10	0	32.9	2.077	4.378	1.699	5.41	6.15	0.491	0.342
Block 4													
Sample 1	1750	1.200	80	30	0	134.7	1.241	2.881	2.227	5.87	7.56	0.635	0.526
Sample 2	1000	0.774	65	20	2.5	58.5	0.568	2.271	3.819	4.97	7.09	0.567	1.032
Sample 3	1750	1.200	50	30	0	71.0	0.516	2.287	4.229	2.33	3.54	0.768	0.87

Sample 4	1750	0.375	80	10	5	47.9	1.958	4.437	2.187	5.22	6.04	0.526	0.41
Sample 5	200	1.200	65	20	0	52.0	0.213	0.898	3.836	5.98	11.58	2.486	1.93
Sample 6	1000	0.375	65	30	0	55.0	1.184	3.286	2.662	4	5.42	0.849	0.943
Block 5													
Sample 1	200	0.774	50	30	0	28.1	4.855	48.012	9.751	4.6	5.62	0.455	0.536
Sample 2	1750	0.774	65	30	5	72.7	0.908	3.225	3.426	4	5.68	0.487	0.402
Sample 3	200	0.774	50	30	0	31.2	2.651	18.444	6.781	3.08	3.79	0.439	0.455
Sample 4	200	0.774	80	10	5	41.6	0.414	4.081	9.614	4.87	7.85	0.565	0.645
Sample 5	200	1.200	50	30	5	31.4	1.777	18.073	10.075	6.17	8.12	0.601	0.622
Sample 6	200	0.375	80	10	0	33.2	3.099	25.094	7.781.	3.2	3.71	0.661	0.548

.

3.2. *Statistical analysis of the dv50*

Table 3. Investigated model parameters with their estimated parameter effects, their corresponding standard error and borders of the 95%-confidence interval and computed p-values for the response dv50-value. Statistically significant output is coloured in orange (|t| < 0.05) and red (|t| < 0.01).

Term	Estimate	Std Error	Lower 95%	Upper 95%	Prob>|t|
Intercept	0.41	0.49	-0.74	1.55	0.4349
Acceleration (g) (50,80)	-1.97	0.24	-2.54	-1.40	<.0001
Breaks during milling (min) (0,5)	0.46	0.28	-0.18	1.11	0.1357
Milling time (min) (10,30)	-1.16	0.23	-1.69	-0.64	0.0009
Bead-suspension ratio (0.375,1.2)	-1.77	0.28	-2.50	-1.04	0.0014
Bead size (µm) (200,1750)	-1.51	0.23	-2.05	-0.97	0.0003
Acceleration (g)*Breaks during milling (min)	-0.48	0.31	-1.21	0.25	0.1622
Acceleration (g)*Milling time (min)	0.64	0.33	-0.43	1.70	0.1512
Acceleration (g)*Bead-suspension ratio	1.44	0.40	-0.09	2.98	0.0566
Acceleration (g)*Bead size (µm)	2.23	0.37	0.55	3.91	0.0301
Breaks during milling (min)*Milling time (min)	0.59	0.48	-0.78	1.96	0.2918
Breaks during milling (min)*Bead-suspension ratio	0.11	0.37	-0.75	0.97	0.7783
Breaks during milling (min)*Bead size (µm)	-0.11	0.29	-0.80	0.57	0.7034
Milling time (min)*Bead-suspension ratio	-0.02	0.42	-1.13	1.09	0.9566
Milling time (min)*Bead size (µm)	0.86	0.26	0.27	1.46	0.0102
Bead-suspension ratio*Bead size (µm)	1.92	0.39	0.98	2.85	0.0021
Acceleration (g)*Acceleration (g)	0.37	0.74	-2.21	2.96	0.6548
Breaks during milling (min)*Breaks during milling (min)	-1.35	0.51	-2.66	-0.04	0.0455
Milling time (min)*Milling time (min)	1.21	0.63	-0.29	2.72	0.0978
Bead-suspension ratio*Bead-suspension ratio	1.45	0.53	-0.17	3.06	0.0660
Bead size (µm)*Bead size (µm)	1.69	0.61	0.24	3.13	0.0278
Acceleration (g)*Bead-suspension ratio*Bead size (µm)	-2.11	0.38	-3.00	-1.21	0.0007

In short, a broad set of parameters were statistically significant for the final median particle size, the dv50-value (p-value < 0.05) (Table 3). Milling time, acceleration, bead-suspension ratio and bead size were critical factors, both as main factor as in most of their two-way interactions (acceleration/bead size, milling time/bead size and bead-suspension ratio/bead size), as illustrated in the broad set of crossing functions in the interaction profiler (Fig. S3). Even with their modest power, some quadratic interactions (breaks during milling and bead size) had a statistically significant outcome. Also, the three-way interaction (acceleration/bead-suspension ratio/bead size) had a statistically significant effect on the final dv50-value.

Acceleration was the most important factor governing the milling process, with a critical parameter estimate of -1.97 (± 0.24). Milling time showed a statistically significant inverse dependence on the dv50-value with a parameter estimate of -1.16 (± 0.23).

Bead-suspension ratio and the bead size were other key variables in the milling process with parameter estimates of -1.77 (± 0.28) and -1.51 (± 0.23), respectively. Surprisingly, the breaks during milling did not have in the provided dataset a statistically significant effect on the final dv50-value.

Even with a modest power of 0.321 and 0.23, the quadratic effects of bead size and breaks during milling were statistically significant with parameter estimates of 1.69 (± 0.61) and -1.35 (± 0.53), respectively. The quadratic term of milling time on the other hand, did not show a statistically significant outcome. Albeit some factors were not considered to be statistically significant, all model terms were included in the predictive model (Model S1), as alluded to above. The accuracy of the generated prediction model was described by the determination coefficient (R^2) and adjusted determination coefficient (R_{adj}^2). As the final determination coefficient of 0.982 only decreased to an adjusted determination coefficient of 0.934, the inclusion of all parameters was well-founded.

3.3. *Statistical analysis of the temperature after milling*

Table 4. Investigated model parameters with their estimated parameter effects, their standard errors, the limits of their 95%-confidence interval and computed p-values for the response temperature after milling. Statistically significant output is coloured in orange (|t| < 0.05) and red (|t| < 0.01).

Term	Estimate	Std Error	Lower 95%	Upper 95%	Prob>|t|
Intercept	58.71	1.14	55.89	61.53	<.0001
Acceleration (g) (50,80)	16.06	0.45	14.96	17.16	<.0001
Breaks during milling (min) (0,5)	-3.33	0.48	-4.48	-2.18	0.0003
Milling time (min) (10,30)	8.56	0.46	7.48	9.64	<.0001
Bead-suspension ratio (0.375,1.2)	12.29	0.61	10.87	13.71	<.0001
Bead size (µm)(200,1750)	13.15	0.53	11.82	14.49	<.0001
Acceleration (g)*Breaks during milling (min)	-1.68	0.57	-3.09	-0.28	0.0263
Acceleration (g)*Milling time (min)	4.55	0.72	2.87	6.22	0.0003
Acceleration (g)*Bead-suspension ratio	5.04	0.79	3.22	6.86	0.0002
Acceleration (g)*Bead size (µm)	3.34	0.72	1.69	4.99	0.0016
Breaks during milling (min)*Milling time (min)	-0.89	0.84	-2.82	1.05	0.3214
Breaks during milling (min)*Bead-suspension ratio	-1.66	0.64	-3.18	-0.13	0.0372
Breaks during milling (min)*Bead size (µm)	-0.70	0.53	-2.01	0.61	0.2338
Milling time (min)*Bead-suspension ratio	2.70	0.77	0.91	4.49	0.0083
Milling time (min)*Bead size (µm)	4.26	0.56	2.95	5.57	<.0001
Bead-suspension ratio*Bead size (µm)	2.33	0.66	0.78	3.88	0.0092
Acceleration (g)*Acceleration (g)	2.72	1.41	-0.52	5.97	0.0889
Breaks during milling (min)*Breaks during milling (min)	0.14	1.18	-2.98	3.25	0.9139
Milling time (min)*Milling time (min)	0.46	1.12	-2.35	3.27	0.6954
Bead-suspension ratio*Bead-suspension ratio	-2.07	1.22	-5.25	1.11	0.1522
Bead size (µm)*Bead size (µm)	-7.56	1.05	-10.17	-4.95	0.0005
Acceleration (g)*Bead-suspension ratio*Bead size (µm)	0.93	0.71	-0.80	2.67	0.2357

Nearly all parameters demonstrated a significant effect on the temperature after milling and thus on the heat generation during IVM (Table 4). This high level of significance is substantiated by the broad operational ranges and the high precision of the temperature measurements. Albeit, it may also indicate the high complexity of the IVM process.

Acceleration was a key contributor to the heat generation with a remarkable parameter estimate of 16.06 (± 0.45). The milling time on the other hand only encompassed a parameter estimate of 8.56 (± 0.46). Other significant key variables were bead size and bead-suspension ratio, with parameter estimates of 13.15 (± 0.53) and 12.29 (± 0.61), respectively. Even in this case, bead size' quadratic effect of -7.56 (± 1.05) was statistically significant. As presumed, breaks during milling had a statistically significant effect on the suspension's final temperature. Albeit, the parameter estimate was only

-3.33 (± 0.48) implying that despite its significance, the model estimate on itself was rather modest as compared to the model estimates of the remaining process parameters. Thus, a temperature rise stayed, even with the inclusion of a periodical five-minute break during milling, inevitable. Hence finetuning of all process parameters remained important.

Almost all two-way interactions had a statistically significant outcome with parameter estimates ranging from circa |2| to |5|. All parameters were included in the predictive model (Model S2). With a R^2 of 0.999 and a R_{adj}^2 of 0.996 (Fig. 2), temperature may be accurately forecasted.

3.4. Statistical analysis of the particle size distribution (dv90, span)

Table 5. Investigated model parameters with their estimated parameter effects, their corresponding standard error and borders of their 95%- confidence intervals including the computed p-value for the response dv90-value. Statistically significant output is coloured in orange (|t| < 0.05) and red (|t| < 0.01).

Term	Estimate	Std Error	Lower 95%	Upper 95%	Prob>|t|
Intercept	-0.24	4.20	-9.93	9.44	0.9554
Acceleration (g) (50,80)	-6.88	1.91	-11.28	-2.48	0.0069
Breaks during milling (min) (0,5)	-0.85	1.98	-5.41	3.72	0.6804
Milling time (min) (10,30)	-2.32	1.84	-6.58	1.93	0.2427
Bead-suspension ratio (0.375,1.2)	-6.43	1.99	-11.01	-1.85	0.0120
Bead size (µm) (200,1750)	-9.13	1.94	-13.60	-4.66	0.0015
Acceleration (g)*Breaks during milling (min)	-0.10	2.44	-5.72	5.53	0.9697
Acceleration (g)*Milling time (min)	1.84	2.11	-3.03	6.71	0.4095
Acceleration (g)*Bead-suspension ratio	0.54	2.33	-4.83	5.91	0.8231
Acceleration (g)*Bead size (µm)	8.86	2.08	4.06	13.66	0.0028
Breaks during milling (min)*Milling time (min)	4.03	2.77	-2.36	10.42	0.1839
Breaks during milling (min)*Bead-suspension ratio	-0.99	2.44	-6.62	4.63	0.6948
Breaks during milling (min)*Bead size (µm)	0.93	2.34	-4.46	6.33	0.7001
Milling time (min)*Bead-suspension ratio	-1.98	2.62	-8.01	4.06	0.4717
Milling time (min)*Bead size (µm)	1.40	2.10	-3.45	6.25	0.5242
Beads-uspension ratio*Bead size (µm)	7.32	2.41	1.75	12.88	0.0163
Acceleration (g)*Acceleration (g)	5.20	4.30	-4.72	15.11	0.2612
Breaks during milling (min)*Breaks during milling (min)	-2.91	4.00	-12.13	6.30	0.4866
Milling time (min)*Milling time (min)	5.33	5.02	-6.26	16.91	0.3199
Bead-suspension ratio*Bead-suspension ratio	0.28	3.80	-8.47	9.03	0.9435
Bead size (µm)*Bead size (µm)	8.52	4.58	-2.05	19.08	0.1001
Acceleration (g)*Bead-suspension ratio*Bead size (µm)	-3.05	2.95	-9.86	3.76	0.3323

In the analysis of the dv90-value, relatively high standard errors were observed and only a handful of factors were statistically significant (Table 5). Due to this high variation unaccounted by the model terms, the dv90 was only shortly described, though the final predictive model (Model S3) was still computed. As expected, the resulting R^2 and R_{adj}^2 were the lowest so far with final values of 0.928 and 0.739, respectively.

Acceleration had, as in the case of dv50, an important impact on the dv90, with a parameter estimate of -6.88 (± 1.91). Other main effects such as bead-suspension ratio and bead size and the two-way interactions acceleration/bead size and bead-suspension ratio/bead size were also statistically significant. The effect of breaks during milling on the other hand was limited.

Table 6. Investigated model parameters with their estimated parameter effects, their corresponding standard error and the borders of their confidence interval (95% confidence interval) including the computed p-value for the response span. Statistically significant output is coloured in orange (|t| < 0.05) and red (|t| < 0.01).

Term	Estimate	Std Error	Lower 95%	Upper 95%	Prob>|t|
Intercept	2.10	1.11	-0.95	5.15	0.1291
Acceleration (g) (50,80)	0.65	0.26	-0.02	1.32	0.0541
Breaks during milling (min) (0,5)	1.16	0.30	0.44	1.88	0.0063
Milling time (min) (10,30)	1.26	0.41	0.24	2.28	0.0233
Bead-suspension ratio (0.375,1.2)	-1.87	0.44	-2.88	-0.85	0.0030
Bead size (µm) (200,1750)	-3.15	0.54	-4.59	-1.72	0.0030
Acceleration (g)*Breaks during milling (min)	1.14	0.34	0.29	1.99	0.0175
Acceleration (g)*Milling time (min)	1.13	0.47	0.05	2.22	0.0423
Acceleration (g)*Bead-suspension ratio	-3.12	0.45	-4.21	-2.03	0.0003
Acceleration (g)*Bead size (µm)	0.39	0.42	-0.61	1.39	0.3885
Breaks during milling (min)*Milling time (min)	2.74	0.54	1.49	3.99	0.0010
Breaks during milling (min)*Bead-suspension ratio	-1.82	0.38	-2.75	-0.89	0.0027
Breaks during milling (min)*Bead size (µm)	-2.38	0.32	-3.18	-1.59	0.0004
Milling time (min)*Bead-suspension ratio	-3.91	0.54	-5.17	-2.66	0.0001
Milling time (min)*Bead size (µm)	-1.98	0.48	-3.17	-0.79	0.0068
Bead-suspension ratio*Bead size (µm)	3.57	0.40	2.63	4.51	<.0001
Acceleration (g)*Acceleration (g)	2.82	0.85	0.83	4.81	0.0118
Breaks during milling (min)*Breaks during milling (min)	0.16	1.20	-3.12	3.44	0.8996
Milling time (min)*Milling time (min)	-1.32	0.67	-3.01	0.37	0.1032
Bead-suspension ratio*Bead-suspension ratio	-1.44	1.15	-4.50	1.62	0.2726
Bead size (µm)*Bead size (µm)	4.81	0.61	3.24	6.37	0.0005
Acceleration (g)*Bead-suspension ratio*Bead size (µm)	1.03	0.42	-0.02	2.08	0.0533

In contrast to dv90s limited set of statistically significant parameters, span produced an extensive list of variables approaching and surpassing the statistical significance of 0.05 (Table 6). Bead size critically impacted the span, indicated by the statistically significant main effect, quadratic effect and two-way interaction with bead-suspension ratio. For a limited set of model parameters, statistical significance could not be proven. The resultant predictive model (Model S4) had a high R^2 and R_{adj}^2 of 0.995 and 0.983, respectively.

4. Discussion

4.1. Application of the stress model

Researchers attempt to predict WBM kinetics and WBM outcomes by process modelling where the stress model suggested by Kwade (Kwade, 1992) and the microhydrodynamic model proposed by Afolabi and co-workers. (Afolabi et al., 2014) are the most widely known. A brief introduction on the stress model is proved below and in the supplementary information (Model S5), nonetheless, interested readers are referred to the original articles presenting these pioneering mechanistic models (Kwade, 1992) (Afolabi et al., 2014).

In the stress model (Kwade, 1992), the process parameters of a stirred media mill are directly linked to the stress applied on the suspension's particles via two central parameters, the stress number (*SN*) and the stress intensity of the grinding media (SI_{GM}). The *SN* is a measure for the number of stress events, and SI_{GM} is the specific energy consumed by a single stress event. This simplification resulted in important caveats. However, it made the model easy to apply and offered easy to understand insights in the milling process. (Kwade and Schwedes, 2002). Accordingly, the question rises if these principles, build upon a stirred media mill, are applicable on the trends observed in the IVM.

In view of the DoE, acceleration was the most important factor impacting the particle size reduction in the IVM. As explained by the stress model (Model S5), the increased acceleration will lead to both an increased intensity of the stress during a milling moment - an increased *SI* - and an increased number of stress moments overall - an increased *SN*. Bead-suspension ratio was another key operation parameter. Increasing the bead-suspension ratio, led to a higher N_{GM} and thus a higher *SN*. This increased number of collisions will naturally lead to a more intense particle size reduction. In a similar manner, the milling time (*t)* led, via an increased N_C, to an increased *SN*. Thus, smaller particles were retrieved, when milling for a longer time. To be more accurate, milling curves are within the literature described by a fast non-linear decrease which eventually stabilise towards the (apparent) grinding limit where the particle size will fluctuate based on the balancing phenomena of grinding, aggregation and crystal growth. (Sommer et al., 2006) (Wang et al., 2013) In this study, the quadratic term of milling time, which would indicate non-linearity, did not show a

statistically significant outcome. Nonetheless, the power of the quadratic term was low and may indicate that in the case of a larger sample size, statistical significance would be evoked. This example explains why power analysis is an important element to consider during DoE analysis. Aside of its effect on the final particle size, milling time importantly impacted the span. Over the milling process, the PSD evolves from a multimodal to a monomodal distribution based on the interplay between particle size reduction, (re)aggregation and recrystallisation (Sommer et al., 2006) and as a result, the span will differ in function of the grinding time.

4.2. The optimal bead size

The common rule, "*the smaller the bead size, the smaller the final particle size*", has already been variously challenged in the field of WBM. (Li et al., 2017), (Peltonen, 2018), (Ghosh et al., 2011) Depending on the process parameters and the suspension properties, the impact of the bead size will differ. (Peltonen, 2018) The literature suggests that an optimal bead size exists within the IVM. This bead size is dependent on the power density and hence dependent on the installed acceleration and bead-suspension ratio (Li et al., 2016b). Nonetheless, this conclusion was based on a one-variable-at-a-time approach which cannot capture interaction effects and hence present conclusive results.

Within this DoE however the existence of the optimal bead size was confirmed. Aside of the main effect, a wide array of two-way interactions proved to be statistically significant. Furthermore, the quadratic effect was, even with a modest power of 0.312, statistically significant indicating the non-linear impact of this process parameter on the final dv50-value.

These previously mentioned two-way interactions could be mechanistically explained. The statistically significant two-way interaction acceleration/bead size could be rationalised by its similar effect on the kinetic energy *(E_{kin})* of the grinding media:

$$E_{kin} = \frac{m\,v^2}{2} \qquad \textit{(Eq. 3)}$$

where E_{kin} *(J)* is kinetic energy, *m (kg)* is the mass of the moving bead and *v (m/s)* is the speed of the moving bead. If the acceleration increased, the velocity of the beads rose, and more kinetic energy was created (Equation 3). Since the velocity of the beads

is squared in E_{kin}'s equation as opposed to the mass, the acceleration could be increased to such extent that the added value of the mass of the grinding media - and so the bead size - to the final E_{kin} becomes negligible.

The statistically significant interaction bead-suspension ratio/bead size can be depicted in the crossing functions in the interaction profiler (Fig. S3). The bead size will influence the number of beads present in a fixed bead-suspension ratio. As the bead size decreases, a higher number of beads may be present in the same bead-suspension ratio but the generated kinetic energy per bead may be lower. This will directly impact the $N_{GM,}$ *SN* and *SI*. As follows, the N_{GM} and *SN* will increase whereas the *SI* will most probably decrease (Model S5). At a low bead-suspension ratio and thus, low input energy, the bigger beads yielded the smallest particles, whilst at a higher bead-suspension ratio, the smallest beads were more favourable (Fig. S4). The reasoning for this counteracting effect may be recognized in the voids in between the beads. At a larger bead size, the voids in-between the beads tend to be larger. By settling herein, bigger API particles could avoid the milling process, leading to an overall larger median particle size.

Lastly, the optimal bead size was substantiated by the statistically significant effect of the three-way interaction (bead-suspension ratio/acceleration/bead size). Normally these more complex multiple-way-interactions are, based on the hierarchy-principle and the sparsity-of-effects-principle omitted out of a DoE. Nonetheless, the significance of this three-way interaction profoundly substantiated the literature suggesting that the optimal bead size was highly correlated to the installed acceleration and bead-suspension ratio. (Li et al., 2016b) As visualised in Fig. S4, at high specific energies such as the acceleration of 80 g, smaller beads yielded smaller API particles. The fitting of the function describing the impact of the bead size at low acceleration was suboptimal. Nonetheless, it cannot be mistaken that at this lower specific energy, larger beads were more advantageous.

Similarly, the dv90 was remarkably influenced by the acceleration as main effect and the two-way interactions acceleration/bead size and bead-suspension ratio/bead size. This could be explained by the interplay between the kinetic energy of the beads, the number of beads and the size of the voids in-between the beads and their dependence on the bead size.

These voids did not only impact the dv50 and dv90 but had an important influence on the span as well. Within these voids, a fairly monodisperse PSD could evade further milling. Consequently, the bead size as both main factor and quadratic effect produced statistically significant parameter estimates of -3.15 (± 0.54) and 4.81 (± 0.61), respectively.

Aside of its effect on the particle size reduction, the bead size critically determined the heat generation in the IVM. Aside of the statistically significant main effect, the statistically significant quadratic effect had a strong presence in the predictive model, with a parameter estimate of -7.56 (± 1.05). Considering its important effect on both particle size and generated heat, the optimisation of the bead size should be a standard step during IVMs process optimisation.

4.3. Cooling the system

The breaks during milling had an important effect on the final temperature of the suspension. Surprisingly, this main effect did not have in the provided dataset a statistically significant effect on the final dv50 and dv90. Hence, every 7.5 minutes, a break of five minutes may be included without constraining the milling process. Intermittent pausing to cool the system was therefore an attractive option to control the temperature during IVM, which would be easy to standardize and scale-up. Nonetheless the model estimate of -3.33 (± 0.48) was quite modest as compared to the model estimate of the other process parameters. Elevated temperatures may have deteriorating effects on the (physico)chemical properties of the compound, the stabilizer and other excipients. Besides, an increased temperature indicate that energy was lost and thus indicate a suboptimal power consumption. To further limit the generated heat, expected temperature may be computed, based on the set process parameters, via the predictive model. Optimization of the process parameters to limit this heat generation afterwards is feasible and highly recommended. Another possibility is to lengthen the break. However, this fell beyond the operational ranges studied in this DoE.

4.4. Method optimization

Table 7. Parameter estimates of all main effects on the different process parameters and calculation of the ratio of the parameter estimated effect on temperature versus the estimated parameter effect on the dv50-value.

Model estimates	Acceleration (g) (50,80)	Breaks during milling (min) (0,5)	Milling time (min) (10,30)	Bead-suspension ratio (0.375,1.2)	Bead size (µm) (200,1750)
dv50	-1.97 (± 0.24)	0.46 (± 0.28)	-1.16 (± 0.23)	-1.77 (± 0.28)	-1.51 (± 0.23)
dv90	-6.88 (± 1.91)	-0.85 (± 1.98)	-2.32 (± 1.84)	-6.43 (± 1.99)	-9.13 (± 1.94)
Temp	16.06 (± 0.45)	-3.33 (± 0.48)	8.56 (± 0.46)	12.29 (± 0.61)	13.15 (± 0.53)
Span	0.65 (± 0.26)	1.16 (± 0.30)	1.26 (± 0.41)	-1.87 (± 0.44)	-3.15 (± 0.54)
Temp / dv50	-8.15	-7.24	-7.38	-6.94	-8.71

In the present study, an imposing array of 22 model parameters and four responses was extensively investigated. In general, all 22 investigated model parameters showed a statistically significant effect on at least one of the four responses, with an exception of the quadratic effects for milling time and bead-suspension ratio. Albeit, the power of these factors was rather modest. Accordingly, they may still play a fair part in one of the responses. All these statistically significant main effects, two-way interactions, quadratic interactions and even three-way interaction marked the complexity of the IVM process.

Nonetheless, the valuable and fast nanosizing potential of IVM and its potential high throughput-screening was illustrated. After ten minutes of grinding, final dv50-values in the lower micron range (Sample 4, Block 2, Table 2) and even submicron range (Sample 2, Block 3 and Sample 4, Block 5, Table 2) could be detected. This particle size reduction as presented by a decrease in dv50, dv90 and span, was strongly associated with a temperature increase (Fig. 3). The large variability depicted at the lowest dv50, dv90 and span, however, indicated that particle size reduction with a controlled heat generation might be attainable.

In the provided datasets, nanonisation seemed to be the most attainable at the highest acceleration, highest bead-suspension ratio and lowest bead size, which is comprehendible as the high acceleration and bead-suspension ratio would install high energy milling for which a smaller bead size is optimal. Even though these settings would maximise the particle size reduction, they would enhance the heat generation as well. In these cases, it might be advantageous to mill for a longer time than to increase the acceleration. Even though they both lead to a temperature increase, their trend towards this heat generation was different (Fig. 4). As suggested in prior work (De Cleyn et al., 2020), the temperature increase in function of acceleration seemed to be more pronounced than the increase in function of milling time. The ratios of the parameter estimate of temperature on dv50-value were calculated and seem to portray a similar picture (Table 7). While the ratio for acceleration presented a value of -8.15,

this change would only be limited to 7.38 in case of the milling time. In a similar manner, an increase in bead-suspension ratio seemed to be a gentler approach for process intensification than acceleration. At high bead-suspension ratios, even mild acceleration lead to appropriate particle size reduction, where dv50-values might reach nanolevels and dv90-value lower microlevels (Sample 1 and 6, block 2, Table 2 and sample 3, block 4, Table 2). A further increase in grinding time would be interesting to explore, but more experimentation is therefore required. Finally, an optimal bead size may be chosen based on the installed acceleration and bead-suspension ratio.

In this regard, method optimization may be supported by the determination of the designs sweet spot via contour plots. The contour plot of the smaller bead size displayed extreme values. At low acceleration and low bead-suspension ratio, the small beads did not have the capability to compensate for the low kinetic energy and a limited particle size reduction occurred. Whilst, at high accelerations and bead-suspension ratios, the high number of small beads and the smaller voids in-between the beads will enhance the particle size reduction (Fig. 5, left). Independent of the set bead size, the temperature showed the same trend. As the acceleration or bead-suspension ratio rose, a higher temperature was attained. (Fig. 5, right). In finding a sweet spot, the two figures may be overlayed. Thus, to attain an extreme particle size reduction with an acceptable temperature increase, a combination of for example a relatively high bead-suspension-ratio, a relatively high acceleration and a relatively small bead size would be advised.

Finally, for a more adequate optimisation, the herein described strong predictive models may be utilised. With these models, JMP® may directly simulate data over the full experimental domain. With flexible desirability functions, best possible conditions may be obtained. Nonetheless, the model is currently further explored and validated for other APIs and process parameters.

5. Conclusions

In this work, an I-optimal design was applied to investigate how five critical process parameters, namely bead size, bead-suspension ratio, milling time, breaks during milling and acceleration, govern IVM in terms of heat generation and particle size reduction. As a result, our understanding of the IVM was improved, which was further strengthened by the application of Kwades stress model (Kwade, 1992). The complexity of the IVM was demonstrated in the wide extent of statistically significant main effects, two-way interactions, quadratic effects and even three-way interaction. The DoE confirmed the existence of an optimal bead size. Intermitting pausing of 7.5 minutes proved to cool down the system without constraining the particle size reduction. However, to keep temperature under control, the remaining process parameters should be optimised as well. In this regard, contour plots and accurate predictive models might be of value, which were generated for the investigated API and process parameter ranges. With these, both particle size and temperature may be for the first time accurately forecasted. For other APIs and process parameters, the model may currently serve as a rule of thumb. Further research is nonetheless required to substantiate these extrapolations.

References

Afolabi, A., Akinlabi, O., Bilgili, E., 2014. Impact of process parameters on the breakage kinetics of poorly water-soluble drugs during wet stirred media milling: A microhydrodynamic view. Eur. J. Pharm. Sci. 51, 75–86. https://doi.org/10.1016/J.EJPS.2013.09.002

Blecher, L., Kwade, A., Schwedes, J., 1996. Motion and stress intensity of grinding beads in a stirred media mill. Part 1 : Energy density distribution and motion of single grinding beads. Powder Technol. 86, 59–68. https://doi.org/10.1016/0032-5910(95)03038-7

de Aguiar, P.F., Bourguignon, B., Khots, M.S., Massart, D.L., Phan-Than-Luu, R., 1995. D-optimal designs. Chemom. Intell. Lab. Syst. 30, 199–210. https://doi.org/10.1016/0169-7439(94)00076-X

De Cleyn, E., Holm, R., Van den Mooter, G., 2020. Exploration of the heat generation within the intensified vibratory mill. Int. J. Pharm. 119644. https://doi.org/10.1016/j.ijpharm.2020.119644

De Cleyn, E., Holm, R., Van den Mooter, G., 2019. Size Analysis of Small Particles in Wet Dispersions by Laser Diffractometry: A Guidance to Quality Data. J. Pharm. Sci. 108, 1905–1914. https://doi.org/10.1016/j.xphs.2018.12.010

Ghosh, I., Bose, S., Vippagunta, R., Harmon, F., 2011. Nanosuspension for improving the bioavailability of a poorly soluble drug and screening of stabilizing agents to inhibit crystal growth. Int. J. Pharm. 409, 260–268. https://doi.org/10.1016/j.ijpharm.2011.02.051

Hagedorn, M., Bögershausen, A., Rischer, M., Schubert, R., Massing, U., 2017. Dual centrifugation – A new technique for nanomilling of poorly soluble drugs and formulation screening by an DoE-approach. Int. J. Pharm. 530, 79–88. https://doi.org/10.1016/j.ijpharm.2017.07.047

Jacob, S., Nair, A.B., Shah, J., 2020. Emerging role of nanosuspensions in drug delivery systems. Biomater. Res. https://doi.org/10.1186/s40824-020-0184-8

Jensen, W.A., 2018. Open problems and issues in optimal design. Qual. Eng. 30, 583–593. https://doi.org/10.1080/08982112.2018.1517884

Kwade, A., 1992. Wet Comminution In Stirred Media Mills - research and its practical application. Powder Technol. 105, 14–20.

Kwade, A., Schwedes, J., 2002. Breaking characteristics of different materials and their effect on stress intensity and stress number in stirred media mills. Powder Technol. 122. https://doi.org/10.1016/S0032-5910(01)00406-5

Leung, D.H., Lamberto, D.J., Liu, L., Kwong, E., Nelson, T., Rhodes, T., Bak, A., 2014. A new and improved method for the preparation of drug nanosuspension formulations using acoustic mixing technology. Int. J. Pharm. 473, 10–19. https://doi.org/10.1016/j.ijpharm.2014.05.003

Li, M., Alvarez, P., Bilgili, E., 2017. A microhydrodynamic rationale for selection of bead size in preparation of drug nanosuspensions via wet stirred media milling. Int. J. Pharm. 524, 178–192. https://doi.org/10.1016/j.ijpharm.2017.04.001

Li, M., Azad, M., Davé, R., Bilgili, E., 2016a. Nanomilling of Drugs for Bioavailability Enhancement: A Holistic Formulation-Process Perspective. Pharmaceutics 8, 17. https://doi.org/10.3390/pharmaceutics8020017

Li, M., Zhang, L., Davé, R.N., Bilgili, E., 2016b. An Intensified Vibratory Milling Process for Enhancing the Breakage Kinetics during the Preparation of Drug Nanosuspensions. AAPS PharmSciTech 17, 389–399. https://doi.org/10.1208/s12249-015-0364-3

Malamatari, M., Somavarapu, S., Taylor, K.M.G., Buckton, G., 2016. Solidification of nanosuspensions for the production of solid oral dosage forms and inhalable dry powders. Expert Opin. Drug Deliv. https://doi.org/10.1517/17425247.2016.1142524

Merisko-Liversidge, E., Liversidge, G.G., 2011. Nanosizing for oral and parenteral drug delivery: A perspective on formulating poorly-water soluble compounds using wet media milling technology. Adv. Drug Deliv. Rev. 63, 427–440. https://doi.org/10.1016/j.addr.2010.12.007

Müller, R., Junghanns, 2008. Nanocrystal technology, drug delivery and clinical applications. Int. J. Nanomedicine 3, 295. https://doi.org/10.2147/ijn.s595

Müller, R.H., Jacobs, C., Kayser, O., 2001. Nanosuspensions as particulate drug

formulations in therapy: Rationale for development and what we can expect for the future. Adv. Drug Deliv. Rev. 47, 3–19. https://doi.org/10.1016/S0169-409X(00)00118-6

Owen, A., Rannard, S., 2016. Strengths, weaknesses, opportunities and challenges for long acting injectable therapies: Insights for applications in HIV therapy. Adv. Drug Deliv. Rev. https://doi.org/10.1016/j.addr.2016.02.003

Peltonen, L., 2018. Design space and QbD approach for production of drug nanocrystals by wet media milling techniques. Pharmaceutics. https://doi.org/10.3390/pharmaceutics10030104

Raasch, J., 1992. Trajectories and impact velocities of grinding bodies in planetary ball mills. Chem. Eng. Technol. 15, 245–253. https://doi.org/10.1002/ceat.270150406

Resodyn acoustic mixers, 2018. No Title, in: Technical InterChange 2018.

Sigfridsson, K., Rydberg, H., Strimfors, M., 2019. Nano- and microcrystals of griseofulvin subcutaneously administered to rats resulted in improved bioavailability and sustained release. Drug Dev. Ind. Pharm. 45, 1477–1486. https://doi.org/10.1080/03639045.2019.1628769

Sommer, M., Stenger, F., Peukert, W., Wagner, N.J., 2006. Agglomeration and breakage of nanoparticles in stirred media mills-a comparison of different methods and models. Chem. Eng. Sci. 61, 135–148. https://doi.org/10.1016/j.ces.2004.12.057

Van Eerdenbrugh, B., Stuyven, B., Froyen, L., Van Humbeeck, J., Martens, J.A., Augustijns, P., Van den Mooter, G., 2009. Downscaling Drug Nanosuspension Production: Processing Aspects and Physicochemical Characterization. AAPS PharmSciTech 10, 44–53. https://doi.org/10.1208/s12249-008-9170-5

Wang, Y., Zheng, Y., Zhang, L., Wang, Q., Zhang, D., 2013. Stability of nanosuspensions in drug delivery, Journal of Controlled Release. Elsevier. https://doi.org/10.1016/j.jconrel.2013.08.006

Fig. 1. Experimental space of the custom designed DoE, including the investigated parameters; breaks during milling (y-axis, left), milling time (y-axis, right), acceleration (x-axis below), bead-suspensions ratio (x-axis above) and bead size (dot size). Every dot represents an experimental run of the DoE. The experimental design space seemed widely covered by the installed experimental runs.

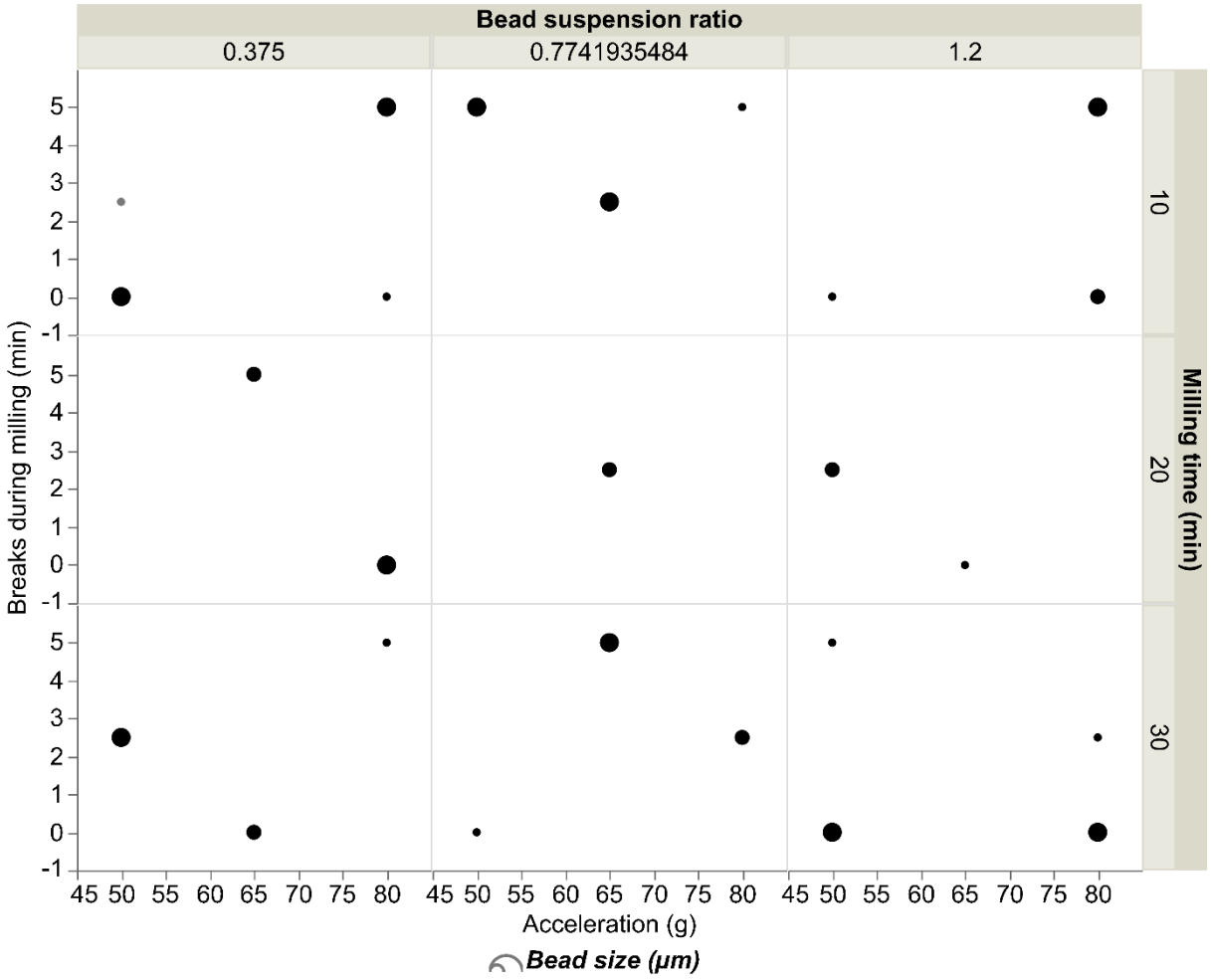

Fig. 2. Strong linear relationship (R^2 of 0.999 and R_{adj}^2 of 0.996) between the predicted temperatures and the actual temperatures of the suspensions after production.

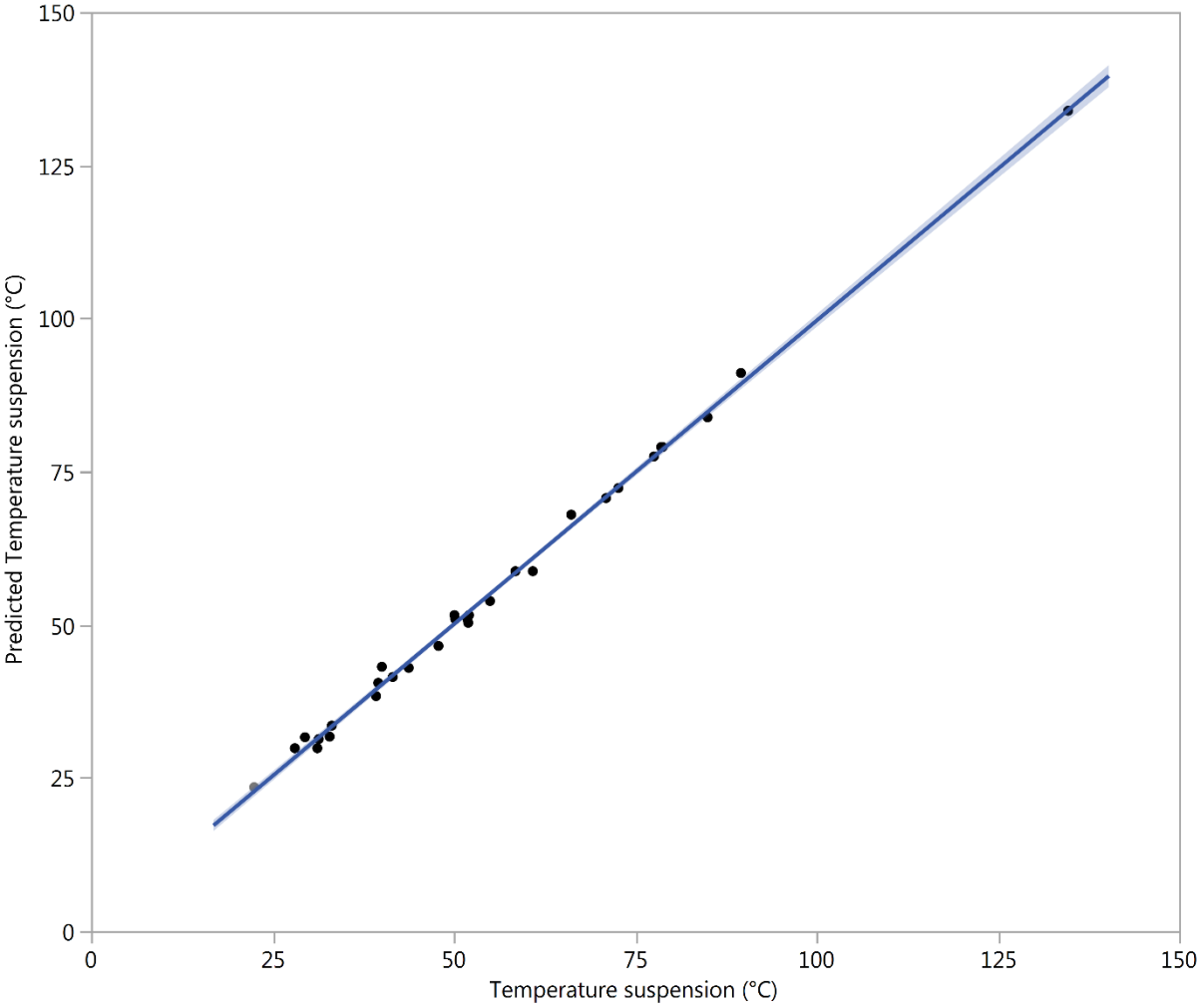

Fig. 3. Measured temperatures in function of the dv90 (left), dv50 (middle) and span (right). Similar trends could be noted where a decrease in particle size or particle size distribution was importantly related to an increase in temperature. Nonetheless, an important variability on the resultant temperature could be detected by the bootstrap confidentiality intervals.

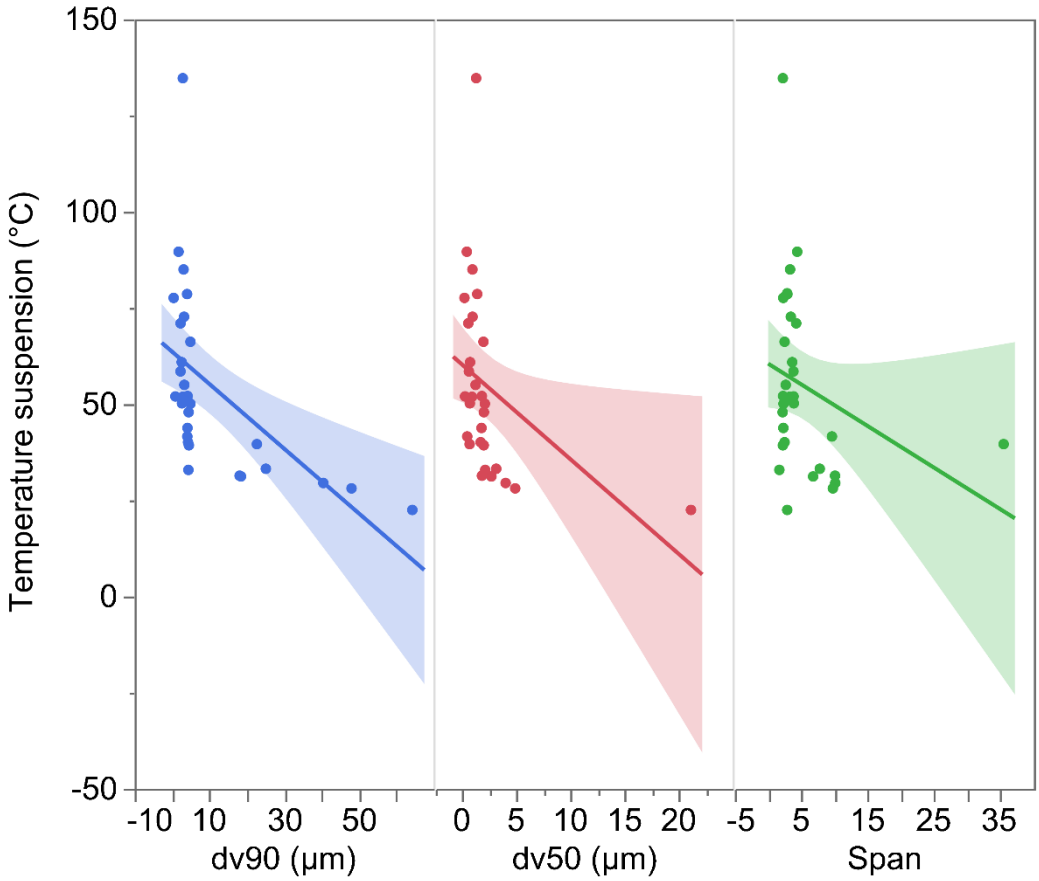

Fig. 4. The temperature trend during continuous milling (breaks during milling = 0 min) when the milling time (left) or the acceleration (right) are investigated. Even though the bootstrap confidence intervals present a certain level of variability, the curve fitting acceleration seems to be steeper than the curve fitting bead-suspension ratio.

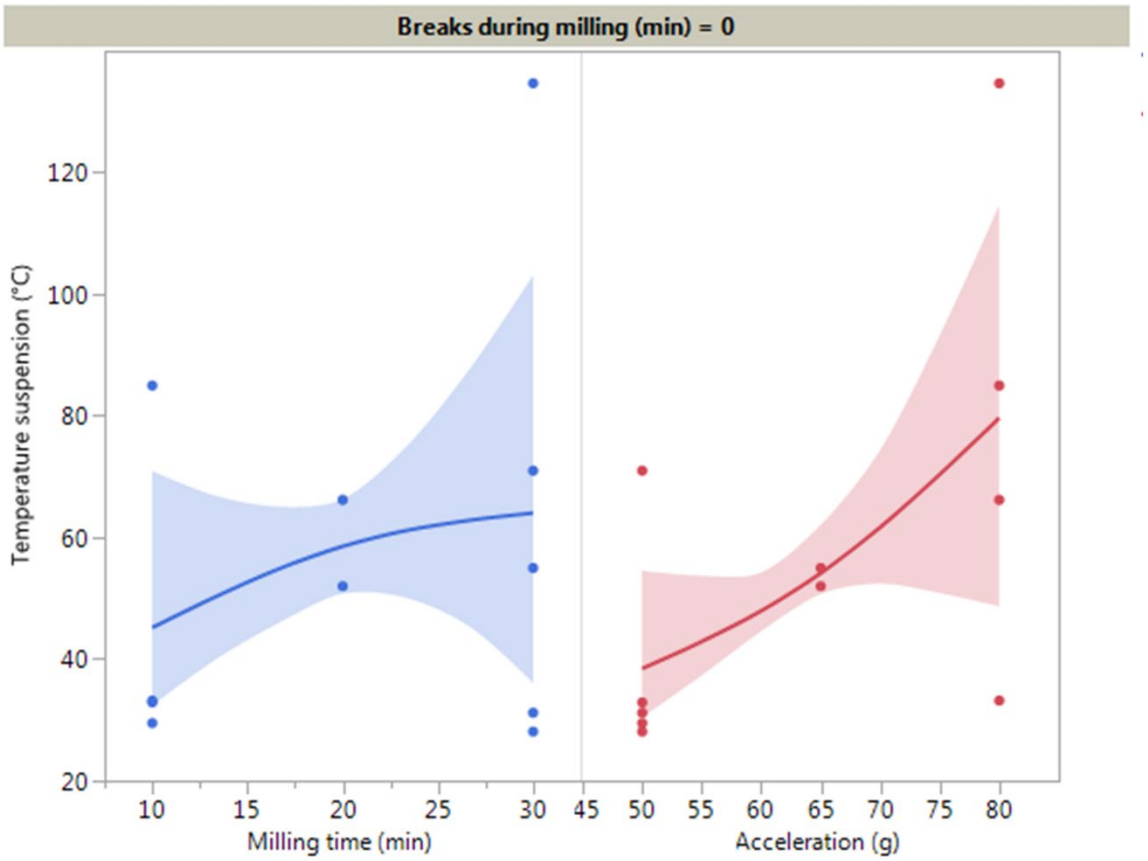

Fig. 5. Contour plots for the dv50 (left) and temperature after milling (right) with as independent variables: bead-suspension ratio (x-axis, below), acceleration (y-axis, left) and bead size (x-axis, above). The settings of the other parameters were variable. The response, dv50 and temperature after milling, was log-transformed and depicted by colour. High values were coloured in red, whereas low values were coloured in blue. Generally, opposite trends may be observed.